Self-assembly of new porous materials

by

Tia Jacobs

Submitted in partial fulfilment of the requirements for the degree

Doctor of Philosophy

at

Stellenbosch University

Department of Chemistry and Polymer Science

Faculty of Science

Supervisor: Prof. L. J. Barbour

Co-Supervisor: Dr. M. W. Bredenkamp

Date: March 2009

elucidated using single-crystal X-ray diffraction. The additional phase is a close-packed polymeric structure which crystallises in the orthorhombic space group *Pbcn*. In this structure (**17**$_{\mathbf{polymer}}$) the L:M:X ratio is identical to that of **17**$_{\mathbf{MeOH}}$, but the ligand adopts an "S" shape, thus precluding formation of the convergent zero-dimensional metallocycle (in which the ligand assumes a "C" shape). This concept is illustrated in Figure 4.9, which show the different possibilities arising from the two major conformations that the ligand can assume. In the structure of **17**$_{\mathbf{polymer}}$, one-dimensional zig-zag polymeric strands propagate along [001] (Figure 4.10a). These strands pack closely such that no solvent is included (Figure 4.10b).

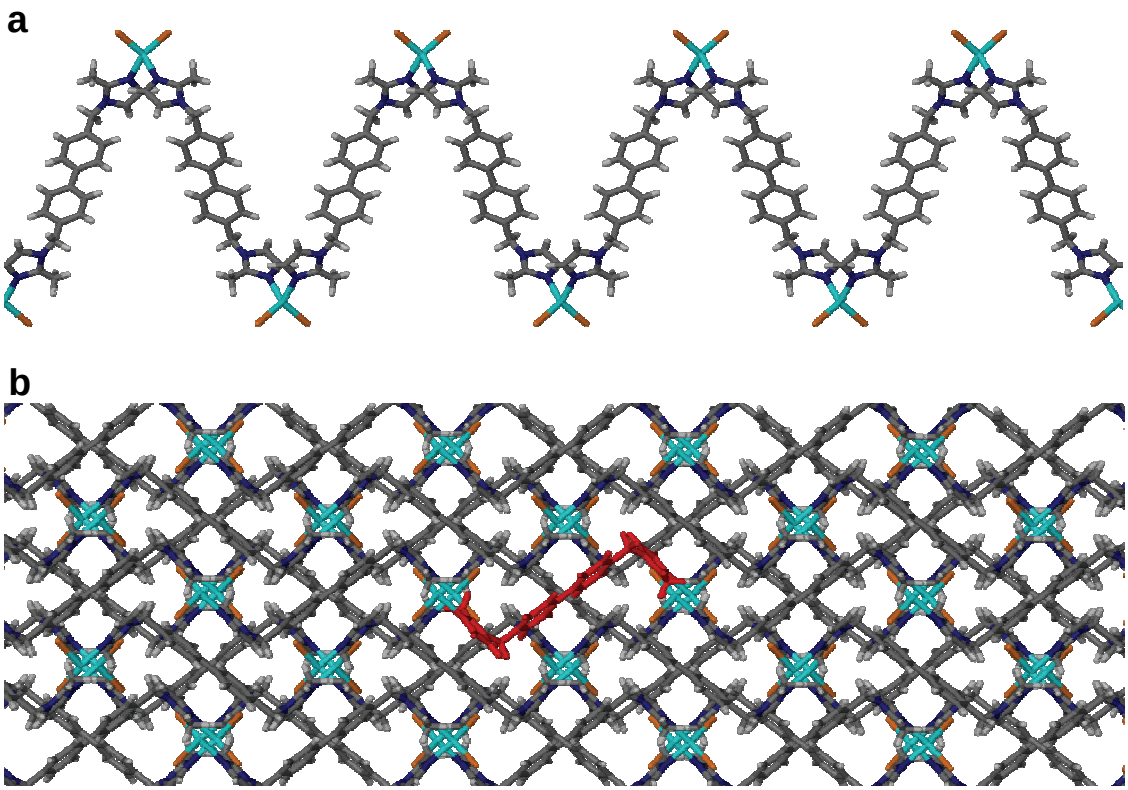

Figure 4.10 **(a)** A perspective view of the 1D strand of **17**$_{\mathbf{polymer}}$ viewed along [100]. **(b)** A view along [001] of **17**$_{\mathbf{polymer}}$; to illustrate the "S"-shape of **L**, the structure is shown in capped-stick and a single ligand (centre) has been coloured red for clarity.

4.2.2 Desolvation of metallocyclic complexes: thermal analysis and single-crystal structures

In order to study the removal of solvent molecules from the host structures, crystals were subjected to thermogravimetric analysis, which showed that desolvation of compounds **13**$_{\mathbf{MeOH}}$ and **14**$_{\mathbf{MeOH}}$ occurs readily, even at room temperature (Figure

4.11a). Although the thermal analysis reported here was conducted using $\mathbf{13}_{\mathbf{MeOH}}$, similar results were obtained for $\mathbf{14}_{\mathbf{MeOH}}$. A theoretical mass loss of 6.4% is expected for two molecules of methanol per cobalt metallocycle, but a slightly lower value 5.6% was obtained thermogravimetrically. This is because guest-loss begins as soon as the crystals are removed from the mother liquor. Using the as-grown crystals and a heating rate of 2.5 ºC per minute, weight-loss due to solvent removal is complete at 63 ºC. Differential scanning calorimetry reveals an endotherm that coincides with the guest-loss process observed by thermogravimetry. To determine whether the single crystals survive the desorption process intact, selected crystals of $\mathbf{13}_{\mathbf{MeOH}}$ and $\mathbf{14}_{\mathbf{MeOH}}$ were heated at *ca* 65 °C for several hours and then inspected under a microscope. Outwardly, the crystals appeared to retain their mosaicity and single-crystal diffraction analysis showed, in both cases, that the ligands undergo conformation changes upon desolvation of the material (Figure 4.12). This results in the formation of an apohost phase in which the cyclic complexes are distorted to yield a more efficiently-packed structure. These guest-free structures $[Co_2\mathbf{L}_2Cl_4]$ and $[Zn_2\mathbf{L}_2Cl_4]$ are referred to below as compounds **13** and **14**, respectively.

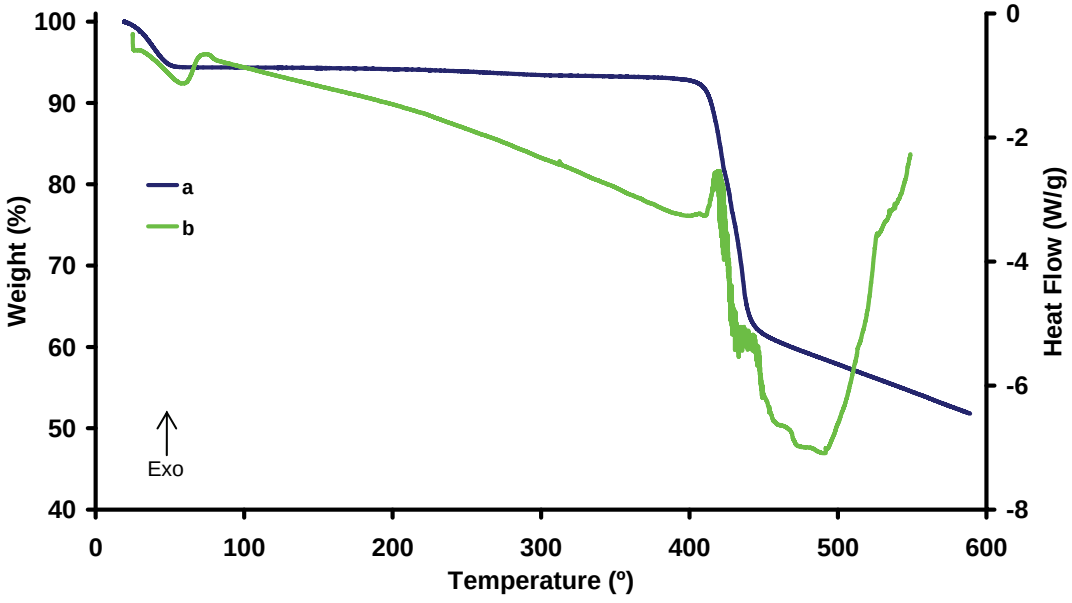

Figure 4.11 **(a)** Thermogravimetric analysis for $\mathbf{13}_{\mathbf{MeOH}}$ showing guest loss starting at room temperature. **(b)** Differential scanning calorimetry indicating a phase change concomitant with guest loss between 20 and 70 ºC.

Figure 4.12 illustrates the changes that occur when $\mathbf{13}_{\mathbf{MeOH}}$ is desolvated to yield **13** (note that identical behaviour is observed for the transformation of $\mathbf{14}_{\mathbf{MeOH}}$ to **14**).

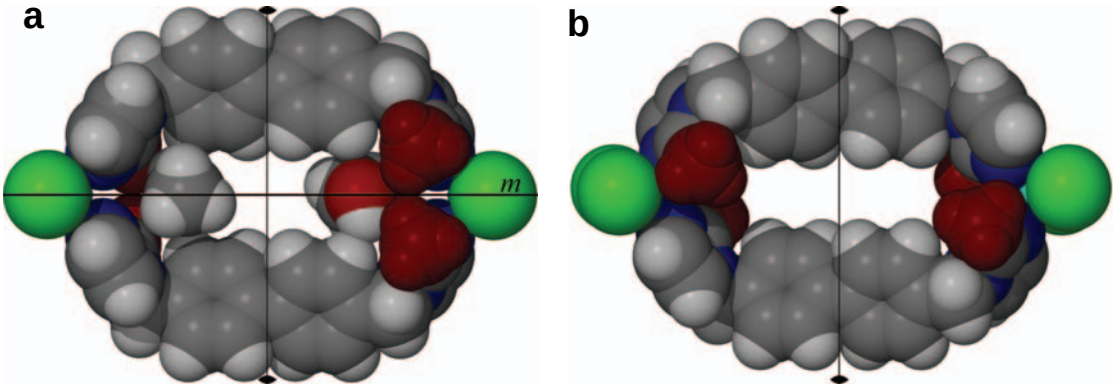

Figure 4.12 Van der Waals projections of the conformation of metallocycles of **(a)** $\mathbf{13}_{\mathbf{MeOH}}$ and $\mathbf{14}_{\mathbf{MeOH}}$ as from solution and **(b) 13** and **14** after desolvation. Molecules are viewed perpendicular to the [100] plane and methyl groups of the 2-methylimidazole moieties are shown in dark red for clarity. Loss of the horizontal mirror plane upon desolvation is illustrated.

The solvated structure (Figure 4.12a) crystallises in the monoclinic space group *C*2/*m*. A mirror plane passes through the two metal centres and the four anions, and a two-fold rotation axis perpendicular to this plane intersects the two C1-C1′ biphenyl bonds (*i.e.* the site symmetry at the centre of the metallocycle is 2/*m*). This requires only a quarter of the metallocycle to be in the asymmetric unit. During desorption, one of the ligands (the one shown on top in Figure 4.12) inverts such that the metallocycle loses its mirror symmetry, but retains its two-fold symmetry (Figure 4.12b). This results in doubling of the size of the asymmetric unit to half of a metallocycle (*i.e.* two halves of a ligand, a metal cation and two halide anions). The desolvated structure conforms to the monoclinic space group *C*2/*c* and the changes in its symmetry result in doubling of the *c*-axis as shown in Figure 4.13.

Twisting of the ligand as a result of desolvation promotes closer packing of the complexes in the apohost structures – *i.e.* the space previously filled by guest molecules is now mostly occupied as a result of more efficient packing of the reconformed metallocycles (Figure 4.14). The conformational change is accompanied by a slight elongation of the metal···metal distance within the metallocycle from 15.881(2) to 16.295(4) Å for **13**, and from 15.964(2) to 16.365(3) Å for **14**. There is also a minor decrease in the N–metal–N angle from 115.6(2)º to 108.7(3)º

a

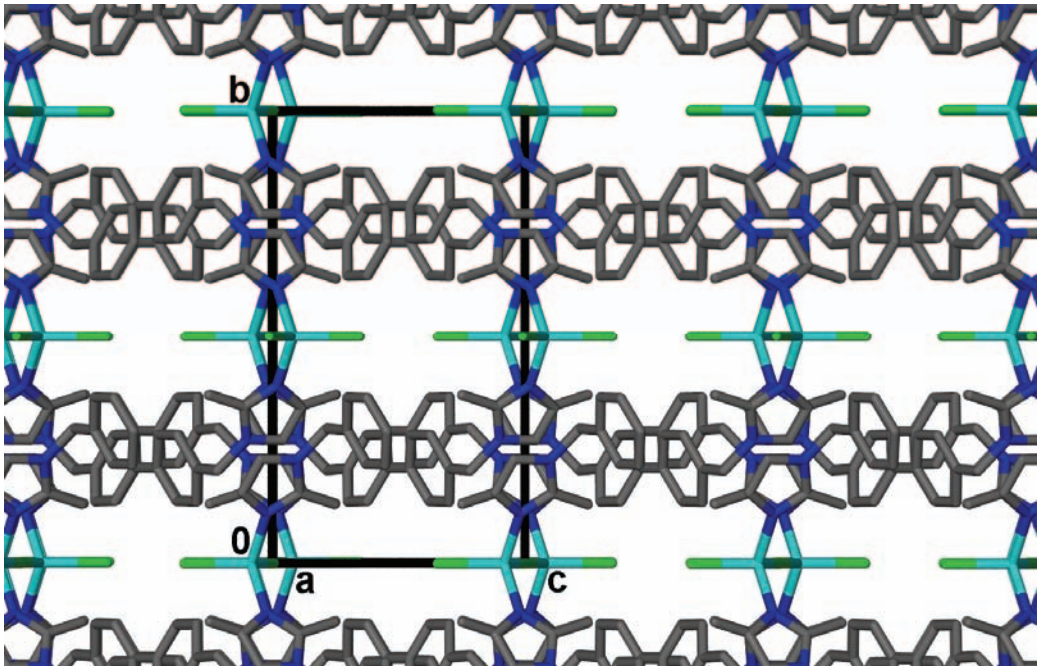

b

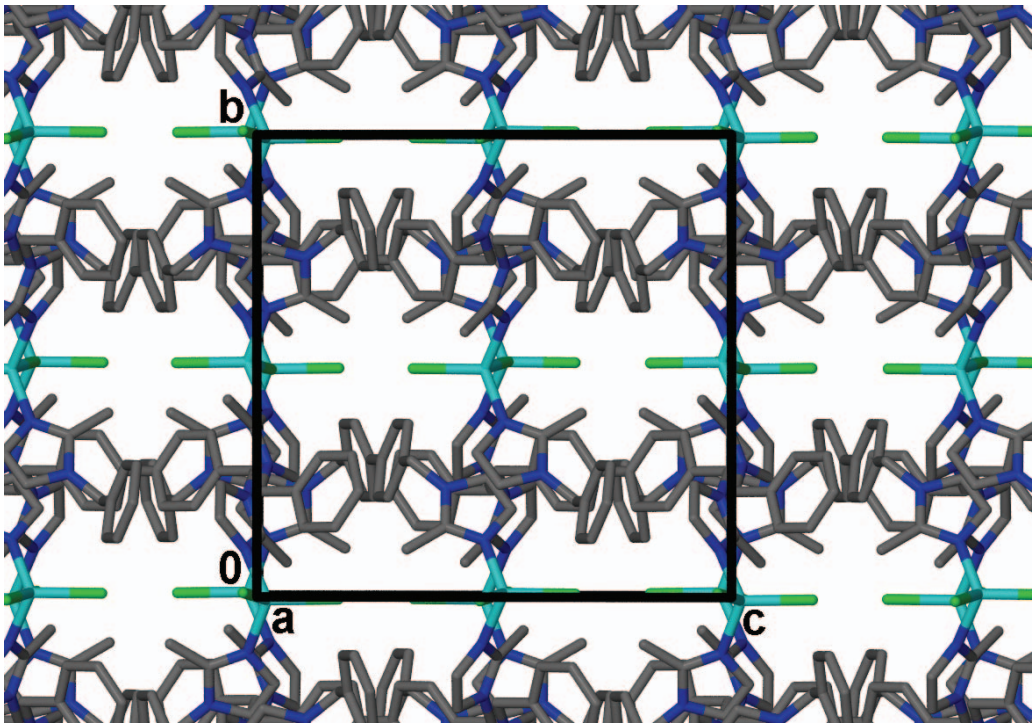

Figure 4.13 **(a)** $\mathbf{13_{MeOH}}$ and **(b) 13** showing doubling of the *c*-axis when the metallocycles rearrange.

for **13**, and from 113.0(3)º to 107.3(2)º for **14**. Crystals of **13** and **14** were immersed in a variety of solvents in an attempt to regain a solvated phase (and the expected corresponding 2/*m* conformation), but these attempts were unsuccessful. It is important to note that, upon ligand rearrangement, significant changes occur within the lattice and one would expect that this would result in enough mechanical strain to cause cracking. Therefore, it is rather surprising that desolvation occurs as single-crystal to single-crystal transformations.

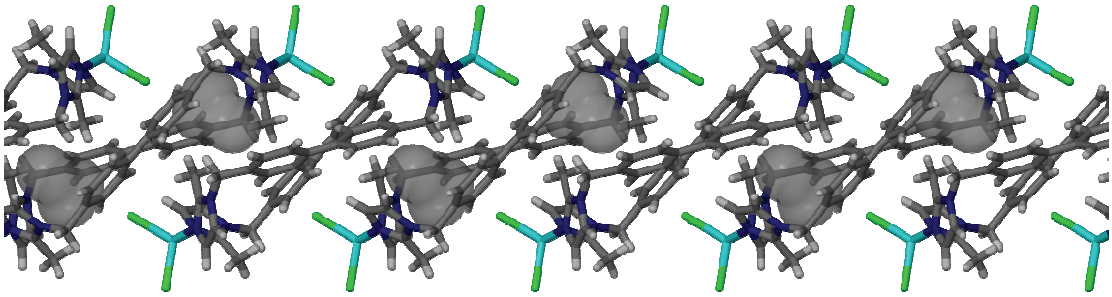

Figure 4.14 Capped-stick projection of the desolvated rearranged metallocycles of **13** and **14** stacked along [001]. The semi-transparent grey surface shows the small void space (r_{probe} = 1.2 Å, volume *ca* 26 Å^3).

Thermal analysis of the inclusion compound $\mathbf{15_{MeOH}}$ (derived from $CdCl_2$) shows that these crystals also lose solvent upon standing at ambient temperature. The thermogram shown in Figure 4.15a shows a 4.9% weight loss (a theoretical value of 5.7% is expected for two equivalents of methanol). In this case, guest removal occurs without a phase change as inferred from the DSC trace (Figure 4.15b) and the coordination complex is stable up to *ca* 400 ºC, after which it decomposes.

Compound $\mathbf{15_{MeOH}}$ loses its guest molecules without concomitant rearrangement of the ligand, thus yielding voids in the apohost phase $[Cd_2\mathbf{L}_2Cl_4]$ (compound **15**). This desolvation process also occurs as a single-crystal to single-crystal transformation and crystallographic studies show that no electron density is present in the pockets previously occupied by the methanol molecules. Two structures were determined at 300 K, one at atmospheric pressure and one under vacuum (the procedure and device are described in section 2.7). Relatively insignificant deviations in the lattice parameters and atomic coordinates of these two structures are observed. The program MSROLL was used to probe the solvent-accessible spaces within the structure. No

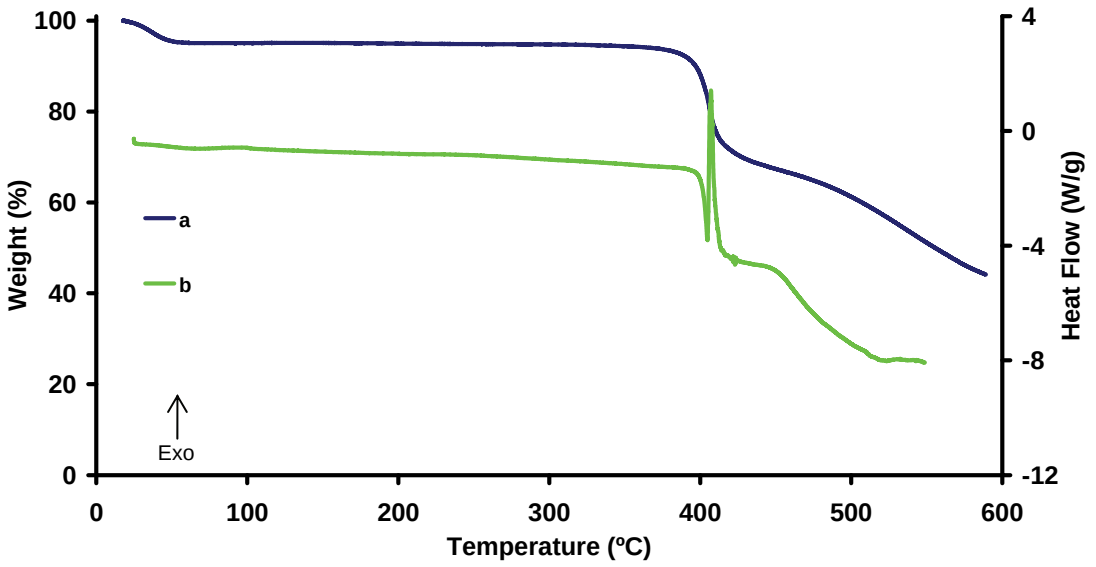

Figure 4.15 **(a)** Thermogravimetric analysis of $\mathbf{15_{MeOH}}$ showing spontaneous guest-loss at room temperature. **(b)** Differential scanning calorimetry does not show signs of a phase change accompanying the guest-loss step.

continuous channels can be mapped through the lattice, but using a probe radius of 1.4 Å, discrete cavities of *ca* 117 $Å^3$ (Figure 4.17a) appear to be present. The unoccupied space in the crystal is estimated to be approximately 10% of the total volume. The reasons for the different behaviours of compounds **13-15**$\mathbf{_{MeOH}}$ upon desolvation are still unclear and a theoretical study is warranted.

Thermogravimetric analysis of $\mathbf{16_{CH2Cl2}}$ and $\mathbf{16_{CHCl3}}$ (Figure 4.16) reveals that these metallocycles lose their guests at onset temperatures of 100 and 140 ºC respectively. The higher temperature needed to desolvate $\mathbf{16_{CHCl3}}$ is attributed to the larger relative size of the guest molecule. In each case, the weight loss corresponds to *ca* one molecule of guest per metallocycle (5.7% for $\mathbf{16_{CH2Cl2}}$ and 7.0% for $\mathbf{16_{CHCl3}}$) with decomposition of the complex occurring after *ca* 270 ºC.

The TGA trace of $\mathbf{17_{MeOH}}$ is similar to that measured for the other methanol solvates, with the crystals losing solvent upon standing under ambient conditions. DSC measurements reveal that the material begins decomposing at *ca* 360 ºC. Desorption of $\mathbf{16_{CH2Cl2}}$ and $\mathbf{17_{MeOH}}$ were also conducted using single crystals and, after structure elucidation, these were shown to be "porous" materials (**16** and **17**). The empty

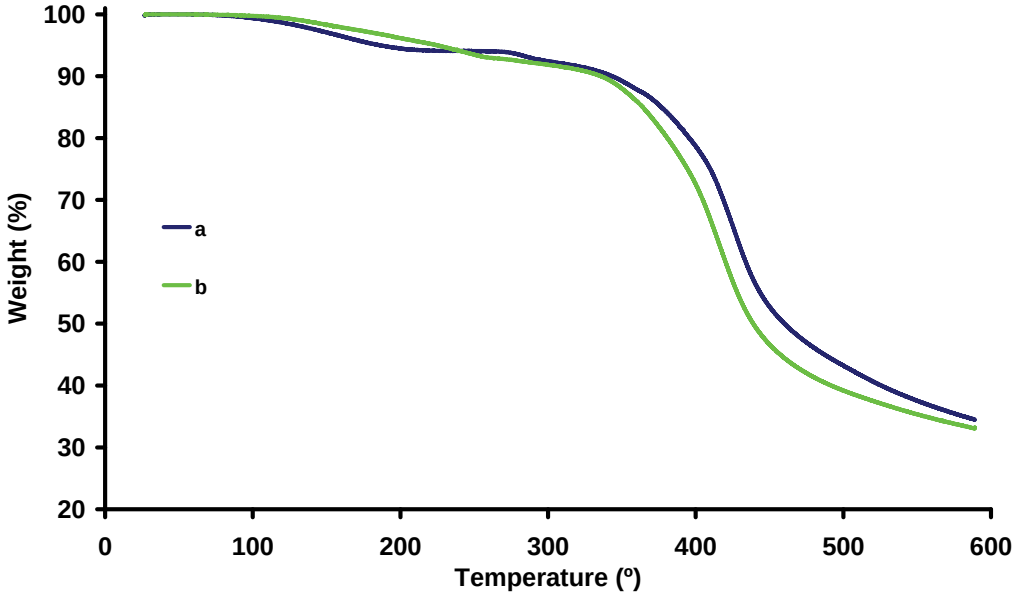

Figure 4.16 Thermograms of **(a) 16**$_{CH2Cl2}$ showing an initial weight loss of 5.7% and **(b) 16**$_{CHCl3}$ showing a weight loss of 7.0%. In both cases this corresponds to *ca* one guest molecule per cavity.

cavities of **16** and **17** are slightly different in shape relative to those of **15**, but the cavity volumes are similar (*ca* 124 and 119 Å^3 for **16** and **17**, respectively). The total unoccupied volume is also *ca* 10% for both **16** and **17** (Figure 4.17).

Having obtained viable systems for gas sorption experiments, the next step was to determine whether they are truly porous in a practical sense. It is worthy of note that, owing to the relatively high densities of these materials (1.46, 1.87 and 1.68 g.cm^{-3} for **15**-**17**, respectively) they would not be considered good candidates for commercial gas storage. However, the size and shape of the cavities of these materials, along with their retention of monocrystallinity, provides us with an excellent opportunity to study gas:solid and gas:gas interactions, and to investigate the effects of changing the anion on their ability to absorb gases.

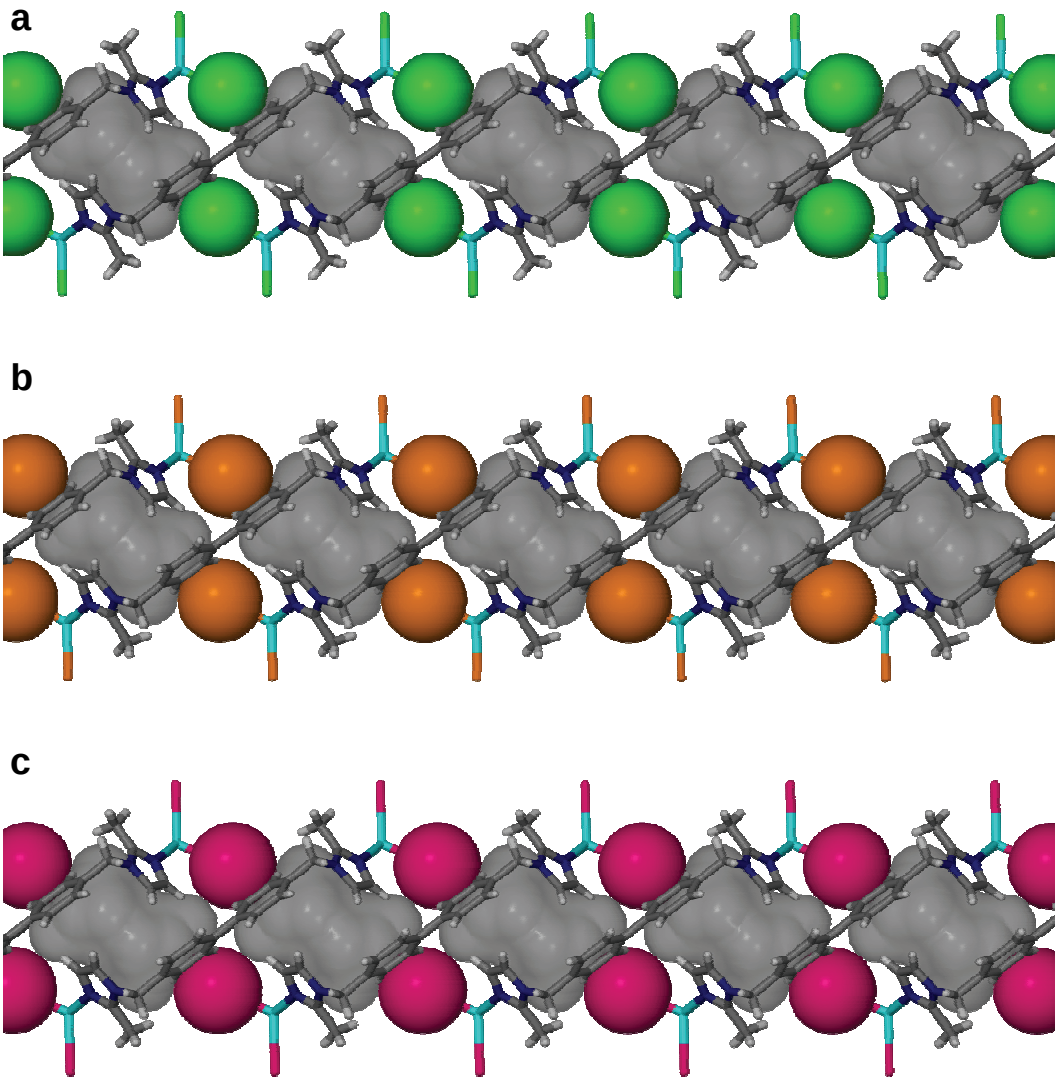

Figure 4.17 Empty voids (semi-transparent grey surfaces) after removal of the guest molecules - structures determined under vacuum. **(a)** Volume *ca* 117 Å^3 for **15**$_{vac}$, **(b)** *ca* 119 Å^3 for **17**$_{vac}$ and **(c)** *ca* 124 Å^3 for **16**$_{vac}$ (r_{probe} = 1.4 Å).

4.2.3 Determination of gas coordinates in crystals

A similar coordination complex system (*i.e.* a [Cu_2**L**$_2Cl_4$] metallocycle) that is permeable to carbon dioxide despite the absence of conventional pores was recently described.[12,13] Although not common, this phenomenon has also been observed for a variety of purely organic host systems.[32-34] Superficial comparison of the molecular volumes of carbon dioxide (CO_2) and acetylene (C_2H_2) reveals that they are approximately the same as that of methanol (*i.e.* 34 Å^3) (Figure 4.4). This suggested that these two gases might be sorbed to also yield a maximum capacity of two guest molecules per void.

After desorbing the guest of **15**$_{\mathbf{MeOH}}$ to produce the empty metallocycle **15,** sorption isotherms were measured for C_2H_2 and CO_2 at 22 ºC (Figure 4.18). The isotherm for C_2H_2 was measured volumetrically and that for CO_2 was measured gravimetrically (see section 4.4.2.2), using powdered samples. Both gases exhibit Type I sorption behaviour, with a slight inflection observed in the isotherm for C_2H_2. Guest occupancies are estimated for each equilibrium pressure from the molar amount of gas absorbed, and are expressed relative to an assumed maximum occupancy of two molecules per cavity. A comparison of the sorption isotherms (shown in Figure 4.18) shows that **15** has a slightly greater affinity for C_2H_2 than for CO_2, *i.e.* at 2 bar the cavities are on average 52% occupied by C_2H_2, as opposed to 45% by CO_2 (these values correspond to an average of 1.04 molecules of C_2H_2 and 0.90 molecules of CO_2 per cavity, respectively). At 12 bar, C_2H_2 and CO_2 reach occupancies of *ca* 95% and 70%, respectively (*i.e.* 1.9 molecules of C_2H_2 and 1.4 molecules of CO_2 per cavity, respectively).

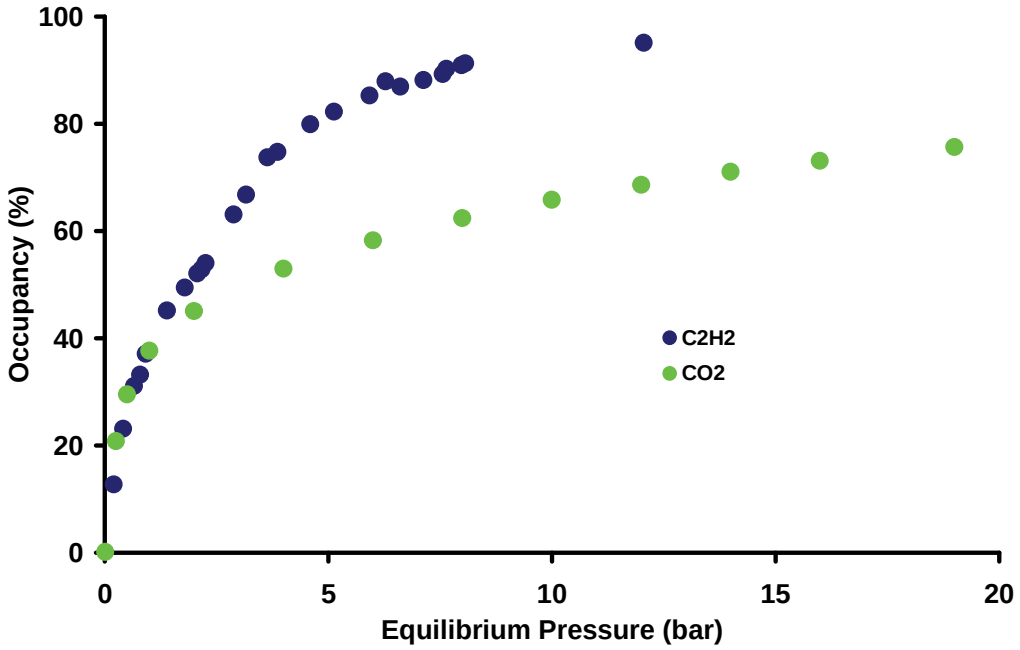

Figure 4.18 Plot showing the sorption of C_2H_2 and CO_2 by **15** at 22 ºC.

Since C_2H_2 and CO_2 are both linear molecules with similar dimensions[25] and boiling points, but inverse electrostatic profiles (Figure 4.4), it is reasonable to presume that differences in their sorption behaviour can be explained in terms of intermolecular host:guest interactions. To gain insight into the supramolecular aspects of sorption in

this particular case, a detailed structural analysis was undertaken using a specially designed gas cell (see section 2.7) which facilitates the collection of a series of X-ray diffraction measurements, each with the crystal exposed to a well-controlled gas pressure. The cell is sufficiently compact that it can be used on a conventional single-crystal diffractometer employing a routine data collection strategy. Using this device, successive intensity data measurements were collected at 22 °C under vacuum and C_2H_2 pressures of 0.5, 1, 2, 4, 6, 8 and 16 bar. Structures will be referred to by **15** subscripted by the pressure and the gas formula (*i.e.* $\mathbf{15_{0.5,C2H2}}$ denotes the structure of **15** determined under a pressure of 0.5 bar of acetylene). The resulting series of structures allows tracking of the incremental pressure-dependent structural changes that accompany the process of gas sorption. Note that X-ray structure analysis only provides a time-averaged view of the unique part of the structure and we cannot therefore observe the state of any individual void.

In principle, the host framework remains unaltered, but undergoes progressive adjustment of its structure to accommodate the step-wise uptake of gas as the pressure is increased. This deformation of the host involves a minor energetic penalty that reaches a maximum of 9.3 kcal.mol^{-1} for $\mathbf{15_{16,C2H2}}$ relative to $\mathbf{15_{vac}}$ (see section 4.4.3). The positions of the C_2H_2 molecules for single- and double-occupancy states were located in difference electron density maps and are shown in Figure 4.19. It is interesting to compare the positions of the guest molecules at 2 and 16 bar (*i.e.* when, presumably, single or double occupancy is maximised, respectively). The C_2H_2 position determined for $\mathbf{15_{2,C2H2}}$ is such that it does not allow room for a second molecule within the confined space of the void. A strong host:guest interaction is inferred since the acetylene molecule never appears to occupy the centre of the cavity, but always lies to either side, even at 50% occupancy when a significant amount of unoccupied space is available. At 16 bar the cavities are almost all doubly occupied (*i.e.* the material is 95% occupied according to sorption analysis) by C_2H_2 molecules and this is also apparent from the structural model. By comparing $\mathbf{15_{2,C2H2}}$ and $\mathbf{15_{16,C2H2}}$ (Figure 4.19a and b, respectively), it is possible to rationalise the structural consequences of inserting a second molecule into the cavity – the first molecule to occupy the cavity is forced to change its position in order to accommodate the second within the confined space. The C–H···Cl$^-$ hydrogen bond is maintained with approximately the same strength as before [having decreased from 6.4 kcal.mol^{-1} to

4.9 kcal.mol^{-1} (see section 4.4.3)], but the preferred orientation of C_2H_2 within the cavity is necessarily altered: the two molecules align themselves across the 2/*m* site such that the C–H···Cl$^-$ angle changes by approximately 25° relative to that in **15$_{2,C2H2}$**. It is interesting to note that the H···Cl$^-$ distances remain approximately the same: 2.585 Å and 2.629 Å in **15$_{2,C2H2}$** and **15$_{16,C2H2}$** respectively.

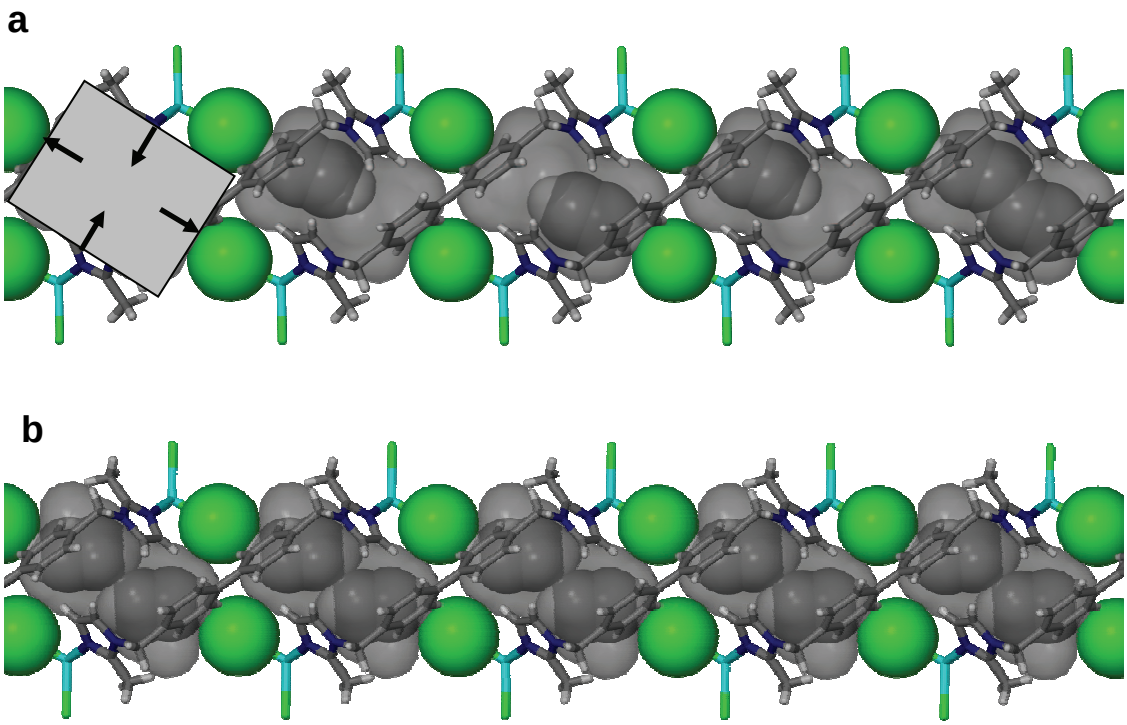

Figure 4.19 Structures of host compound **15** resulting from acetylene sorption. The cavities are shown as semi-transparent grey surfaces with the host metallocycles in capped-stick representation. The chloride anions and the acetylene molecules are shown in space-filling representation to illustrate the C–H···Cl$^-$ interaction. **(a)** The C_2H_2 molecules are disordered over two positions in the structure determined at 2 bar (compound **15$_{2,C2H2}$**) and each cavity is occupied by approximately one molecule of C_2H_2. The single gas molecule is situated at either end of the void and is stabilised in that position by the formation of a H–C≡C–H···Cl$^-$ hydrogen bond (C···Cl$^-$ = 3.51(5) Å). The C_2H_2 molecule is approximately collinear with the Cl···Cl vector across the void, and ∠C–H···Cl$^-$ = 170.3°. Owing to the presence of 2/*m* site symmetry in the centre of the cavity, the C_2H_2 molecule is disordered over two equivalent positions and the model therefore shows overlapping molecules, indicating that either (but not both) of the positions can be occupied at any given moment. **(b)** In **15$_{16,C2H2}$** the cavities are almost fully occupied, *i.e.* each accommodates two molecules of C_2H_2. The H–C≡C–H···Cl$^-$ hydrogen bonds are maintained (C···Cl$^-$ = 3.41(2) Å) but, relative to the structure of **15$_{2,C2H2}$**, the C_2H_2 molecules are required to tilt in order to accommodate one another (∠C–H···Cl$^-$ = 142.1°).

Figure 4.19b shows that the two C_2H_2 molecules are in van der Waals contact with one another and they occupy the available void volume (146 Å^3) with a combined

packing efficiency of approximately 48%. During the process of gas uptake, the average size and shape of the cavity changes (this is most likely a dynamic process for each individual void, even during equilibrium) with the void volume increasing smoothly from 117 Å^3 for **15**$_{vac}$ to 134 Å^3 for **15**$_{2,C2H2}$ to 146 Å^3 for **15**$_{16,C2H2}$. As the pressure is increased from vacuum to 16 bar the void, which can be imagined as a rectangle (Figure 4.19a), stretches along its major dimension and narrows across its minor dimension. The Cl···Cl distance measured across the cavity increases by 11% overall (*i.e.* from 10.645(5) Å to 11.849(8) Å) while the Cd···Cd distance across the cavity contracts by 9% (*i.e.* from 9.4456(15) to 8.586(3) Å). These stepwise changes in the Cl···Cl distance and crystallographic β-angle (which are related to one another and to the Cd···Cd distance) are depicted in Figure 4.20. Furthermore, the "gate" between two neighbouring voids (defined by two Cl^- ions) narrows with increasing pressure, such that the Cl···Cl distances decrease overall from 5.770(5) Å to 5.084(10) Å.

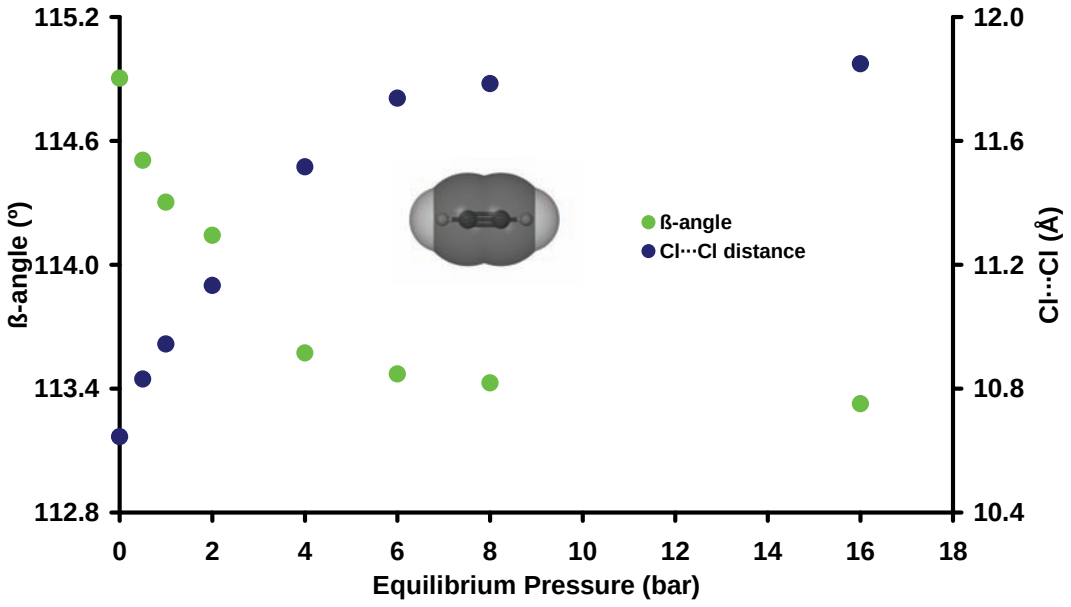

Figure 4.20 The β-angle and Cl···Cl distance undergo significant changes when C_2H_2 is absorbed by **15**. These structural parameters are derived from single-crystal diffraction methods and are plotted as a function of the equilibrium pressure.

In rationalising the process of C_2H_2 uptake, it is useful to consider that any individual cavity can only exist in one of three possible states at any given moment during either the sorption or the equilibrium process: the void can be empty or it can be occupied by either one or two gas molecules. It is reasonable to presume that these three states

interchange rapidly with one another as gas molecules are passed between neighbouring cavities, and that the probability of each state is a constant at equilibrium for a given pressure. We also presume that between 0 and 2 bar the empty and single occupancy states most likely predominate, and that between 2 and 16 bar the single and double occupancy states are more likely (see section 4.2.6 for further discussion).

In order to adequately describe the series of structures in which the host framework remains almost constant and only the C_2H_2 occupancy changes, reasonable crystallographic models are necessary for the guest molecules. It is important to assign correct site occupancy factors to the gas molecules at each pressure, but refinement of site occupancy factors does not yield reliable values when the displacement parameters are also subjected to refinement. Although it is possible to use the independently measured sorption data in order to obtain average occupancy values for the gas molecules, the electron count within the void space [obtained using the program SQUEEZE[35]] can also provide such information. A plot of electron count occupancies against pressure shows that these values are in good agreement with those obtained from gas sorption measurements (Figure 4.21). In order to model the series $\mathbf{15_{0.5,C2H2}}$ to $\mathbf{15_{16,C2H2}}$ crystallographically, the structures were refined by constraining the site occupancy factors of the C_2H_2 molecules such that they were consistent with the values determined from the electron counts within the voids. We note that, in the absence of gravimetric or volumetric sorption data, the electron count method may serve as a means of measuring occupancy at specific pressure while simultaneously providing valuable structural information with regard to the equilibrium structures obtained during the process of gas sorption. In addition, when trying to obtain gas sorption data, sample purity is essential and producing the desired amount of sample necessary for quantitative experiments can often be problematic. This method can serve to screen materials for their gas sorption capability, without the tedious and time-consuming process of producing large samples with high phase purity.

The interaction of CO_2 with the host framework of **15** was also investigated. In a preliminary study, a crystal of **15** was mounted in the gas cell (section 2.7) and the structure determined at 295 K and under 10 atmospheres of carbon dioxide. The

carbon dioxide could not be modelled owing to substantial thermal motion, although it was possible to locate diffuse electron density within the cavity. The structure was then redetermined under the same carbon dioxide atmosphere but at 233 K (designated as $\mathbf{15}_{\mathbf{CO2}}$). Under these conditions, it was possible to model the positions of the CO_2 molecules, which were located within the discrete pockets formed by the doughnut-shaped molecules (Figure 4.22).

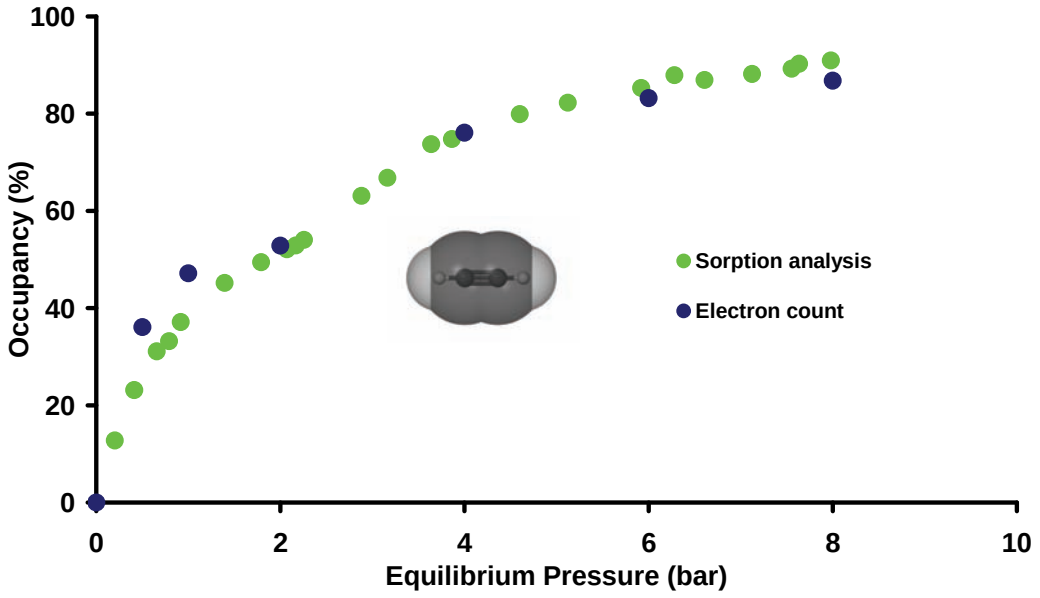

Figure 4.21 Gas sorption isotherms of acetylene by **15** at 22 ºC. The isotherms determined using volumetric gas sorption experiments and the electron count method (SQUEEZE) appear to agree well.

Two CO_2 molecules (each at approximately full occupancy – *i.e.* 43.4 electrons of the expected total of 44 electrons for two CO_2 molecules) were located within each cavity. When occupied by the gas molecules, the void increased significantly in volume to *ca* 145 $Å^3$ (from *ca* 117 $Å^3$ determined for the vacuum structure - r_{probe} = 1.4 Å in both cases). It is interesting to note how the symmetry-equivalent carbon dioxide molecules are aligned within the cavity – their orientations are almost perpendicular to that of C_2H_2 in $\mathbf{15}_{\mathbf{16,C2H2}}$. As might be expected from chemical intuition, the electropositive carbon atom is situated closest to the chloride anion, thus shielding the electronegative oxygens from the anion. The C···Cl^- distance is 3.38(2) Å, with the sum of van der Waals radii being 3.5 Å, suggesting a slight intermolecular interaction between host and guest. In contrast to $\mathbf{15}_{\mathbf{C2H2}}$, there is no

hydrogen bond to stabilise the host:guest adduct; instead, there exists only a weak electrostatic interaction between the positively charged carbon atom of CO_2 and the negatively charged chloride anion of the host. The energy calculated (see section 4.4.3) for the interaction between CO_2 and a simplified $CdCl_2(NH_3)_2$ model compound (where CO_2 is orientated in the same manner as in **15$_{CO2}$**) is 3.7 kcal.mol^{-1} weaker than for the corresponding model of C_2H_2 in **15$_{2,C2H2}$**. This difference presumably accounts for the greater degree of disorder of CO_2 at room temperature.

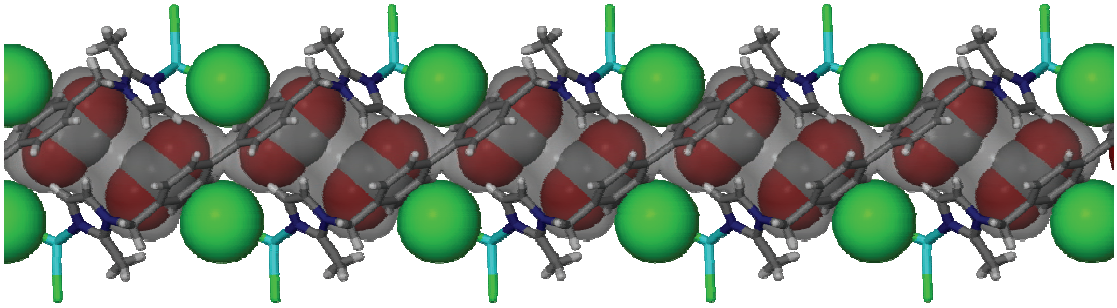

Figure 4.22 Structure of **15$_{CO2}$** determined at -40 ºC under a pressure of 10 bar of CO_2. The guest-accessible cavities are shown as semi-transparent grey surfaces with the host metallocycles and neighbouring carbon dioxide molecules shown in capped-stick representation. The chloride anions forming the floor and roof of the mapped cavity are shown in space-filling representation along with the CO_2 molecules. In contrast to the structures with C_2H_2, the CO_2 molecules are positioned at approximately right angles relative to the Cl···Cl vector across the cavity and form a weak $C(\delta^+)\cdots Cl^-$ interaction with the host complex. The volume of each guest-accessible void is approximately 145 Å^3.

A series of X-ray diffraction measurements was conducted at 22 °C under CO_2 pressures of 0.5, 1, 2, 4, 6, 8, 10, 12 and 14 bar (hereafter the structures are designated as **15$_{05,CO2}$** to **15$_{14,CO2}$**). None of these structures yielded reliable atomic coordinates for the CO_2 molecules, reinforcing the notion that the gas molecules experience significant dynamic displacement at room temperature. Nevertheless, it was still possible to determine the CO_2 occupancies using the electron count method (*i.e.* the program SQUEEZE). From the occupancy data and crystal structures, valuable information could be gained that relates the deformation of the host framework to guest occupancy. Figure 4.23 shows two lattice parameters (Cl···Cl distance and β-angle) that reliably describe the conformational change as a function of gas pressure. The host deformation in response to carbon dioxide uptake is not as significant as for acetylene, suggesting that the orientation imposed on CO_2 does not require as significant a structural change as that imposed on C_2H_2. At 22 ºC the gas molecules